Journal of Energy

VOLUME 74 Number 4 | 2025

journal homepage: http://journalofenergy.com/

Adaptive PWM Control and Dynamic Switching Frequency for Leakage Current Suppression and THD Control in 3-Level NPC Inverters

Mohammed Moyed Ahmed

Summary — **This paper presents an adaptive operation algorithm for 3-level Neutral Point Clamped (NPC) grid-connected inverters that simultaneously addresses leakage current suppression and total harmonic distortion (THD) control in transformerless photovoltaic (PV) systems. The proposed approach integrates intelligent Pulse Width Modulation (PWM) method selection with dynamic switching frequency optimization to achieve optimal inverter performance under varying operating conditions. The algorithm employs a hierarchical control structure where high-level decisions regarding PWM method selection between Phase Disposition (PD) and Phase Opposition Disposition (POD) PWM are made based on real-time leakage current measurements, while low-level switching frequency adjustments using perturbation and observation (P&O) technique maintain acceptable THD levels. Comprehensive PSIM simulation validation demonstrates that the algorithm achieves up to 40% reduction in leakage current under fault conditions while maintaining grid current THD below 3.5%, meeting international safety and power quality standards. The algorithm's response time of 0.5 seconds for leakage current threshold violations and convergence within 1.5-2.0 seconds for THD optimization provides adequate protection for safety applications. The software-based solution requires no additional hardware components, making it suitable for both new installations and retrofit applications in commercial inverter systems. The demonstrated performance under realistic fault conditions and grid disturbances confirms the algorithm's practical viability for transformerless PV inverter applications..**

Keywords — **3-level NPC inverter, adaptive control, leakage current suppression, total harmonic distortion (THD), Phase Opposition Disposition (POD) PWM, common mode voltage (CMV), grid-connected inverters, power quality, switching frequency optimization.**

I. Introduction

The rapid expansion of renewable energy systems and the increasing demand for high-efficiency power conversion have positioned multilevel inverters as critical components. This is particularly evident in modern gridconnected applications [1]. Among various multilevel topologies, the three-level Neutral Point Clamped (NPC) inverter has emerged as a predominant choice for mediumvoltage applications. This predominance stems from its superior power quality characteristics, reduced voltage stress on switching devices, and lower electromagnetic interference. These advantages are significant when compared to conventional two-level inverters [2]. The commercial deployment of 3-level NPC inverters in grid-connected systems requires stringent compliance with international safety and power quality standards, including IEEE 1547, IEC 61727, and VDE-AR-N 4105 [3], [4], [5]. These standards impose strict limitations on leakage current, typically restricting it to less than 300 mA for photovoltaic systems, and mandate grid current Total Harmonic Distortion (THD) to remain below 5%. However, achieving consistent compliance with these standards throughout the inverter's operational lifetime presents significant challenges, particularly when considering the influence of external factors such as parasitic capacitances, cable aging, environmental conditions, and grid impedance variations [6].

Leakage current in grid-connected inverters primarily originates from Common Mode Voltage (CMV) fluctuations, which create current paths through parasitic capacitances between the photovoltaic panels and ground. This phenomenon not only poses safety risks but can also lead to electromagnetic interference, reduced system efficiency, and accelerated degradation of system components [6]. The magnitude of leakage current is significantly influenced by installation-specific factors including cable length, mounting configuration, humidity levels, and ground conditions, making it difficult to predict and control using conventional fixed-parameter approaches [8], [9].

Simultaneously, maintaining acceptable grid current THD levels becomes increasingly challenging as inverters operate under varying load conditions, grid voltage distortions, and component parameter drifts due to aging [10]. The trade-off between leakage current suppression and power quality maintenance represents a fundamental challenge in inverter design, as methods that effectively reduce CMV often compromise harmonic performance and vice versa.

Traditional approaches to address these challenges have primarily focused on either hardware-based solutions, such as additional filtering components and transformer isolation, or software-based methods involving advanced PWM techniques [11]. Hardware solutions, while effective, significantly increase system cost, size, and complexity, making them less attractive for commercial applications [12]. Software-based approaches, particularly those involving PWM modifications, offer more cost-effective solutions but often require careful optimization to balance multiple performance objectives [13], [14].

(Corresponding author: Mohammed Moyed Ahmed)

Mohammed Moyed Ahmed is with the Jawaharlal Nehru Technological University Hyderabad, Hyderabad, India (e-mail: mmoyed@gmail.com)

Mohammed Moyed Ahmed, Adaptive PWM Control and Dynamic Switching Frequency for Leakage Current Suppression and THD Control in 3-Level NPC Inverters, Journal of Energy, vol. 74 Number 4 (2025), 3–13
https://doi.org/10.37798/2025744721

Recent advancements in digital signal processing capabilities and real-time monitoring systems have opened new possibilities for adaptive inverter control strategies that can dynamically respond to changing operating conditions [15], [16]. These intelligent control approaches can potentially overcome the limitations of fixed-parameter methods by continuously optimizing inverter operation based on real-time measurements of critical parameters [17], [18].

This paper addresses the aforementioned challenges by proposing an adaptive operation algorithm for 3-level NPC inverters that intelligently balances leakage current suppression and THD control without requiring additional hardware components. The key contributions of this work include:

1. Development of an adaptive PWM method selection algorithm that dynamically switches between conventional Phase Disposition (PD) and Phase Opposition Disposition (POD) PWM based on real-time leakage current measurements.
2. Implementation of a Perturbation and Observation (P&O) based switching frequency control mechanism that optimizes grid current THD while minimizing switching losses.
3. Design of a comprehensive control framework that integrates leakage current monitoring, THD calculation, and decision-making logic for autonomous inverter operation.

The proposed algorithm offers a practical and costeffective solution for commercial 3-level NPC inverter systems, enabling robust performance under varying environmental and grid conditions while maintaining strict compliance with international safety and power quality standards.

The remainder of this paper is organized as follows: Section II reviews related work in multilevel inverter control and PWM techniques. Section III presents the detailed methodology of the proposed adaptive algorithm. Section IV describes the simulation setup and validation results. Section V discusses the implications and limitations of the proposed approach. Finally, Section VI concludes the paper and outlines future research directions.

II. Related Research

The mitigation of leakage current in grid-connected inverters has been extensively studied, with approaches broadly categorized into hardware-based and softwarebased solutions. Hardware-based methods primarily involve the use of isolation transformers, commonmode chokes, and additional filtering circuits [19], [11]. While transformerless inverters offer higher efficiency and reduced cost, they are more susceptible to leakage current issues, driving the need for innovative topological solutions [20], [21]. Several specialized inverter topologies have been proposed to address leakage current concerns, including the H5 topology by SMA Solar Technology, the HERIC (Highly Efficient and Reliable Inverter Concept) topology, and various NPC-based topologies such as the conergyNPC and H-bridge NPC variants [22], [23]. However, hardware modifications often increase system complexity and cost, motivating extensive research into softwarebased approaches, particularly focusing on PWM strategy modifications.

Pulse Width Modulation strategies for Common Mode Voltage (CMV) reduction represent the fundamental software based approach to leakage current suppression. These strategies can be classified into zero CMV methods, reduced CMV methods, and CMV compensation techniques. Zero CMV methods, such as Remote State PWM (RSPWM) and Near State PWM (NSPWM), completely eliminate CMV by using only voltage vectors that produce zero common-mode voltage [24]. Although theoretically attractive, these methods often result in poor harmonic performance and a limited linear modulation range. Reduced CMV methods represent a compromise between CMV suppression and power quality, with the Phase Opposition Disposition (POD) PWM method gaining attention for its ability to significantly reduce CMV by up to 50% compared to conventional Phase Disposition (PD) PWM, albeit with some degradation in output harmonic content. Recent research has explored advanced PWM techniques such as Discontinuous PWM (DPWM) methods and hybrid modulation strategies [25], [26], [27].

Total Harmonic Distortion (THD) control in multilevel inverters has been addressed through various approaches, including selective harmonic elimination, space vector modulation optimization, and adaptive switching frequency control. Selective Harmonic Elimination PWM (SHEPWM) techniques calculate specific switching angles to eliminate low-order harmonics but are computationally intensive and may not be suitable for real-time applications [28]. Space Vector Modulation (SVM) approaches offer better harmonic performance compared to carrierbased methods and provide additional degrees of freedom for optimization through advanced techniques such as the Nearest Three Vector (NTV) approach and virtual space vector concepts developed specifically for multilevel inverters. Adaptive switching frequency control has emerged as a promising approach for dynamic THD optimization, with Liu et al. [29] proposing a variable switching frequency control method that adjusts based on load conditions, and Wang et al. [30] developing intelligent optimization algorithms using machine learning techniques.

Recent research trends have focused on integrated control strategies that simultaneously address multiple performance objectives through multi-objective optimization approaches using genetic algorithms, particle swarm optimization, and other metaheuristic methods [33], [34]. Ahmed et al. [35] proposed a comprehensive control framework for 3-level NPC inverters that integrates neutral point voltage balancing, harmonic minimization, and CMV reduction using real-time optimization algorithms. Model Predictive Control (MPC) techniques have gained attention for multilevel inverter applications due to their ability to handle multiple constraints and objectives simultaneously, with Finite Control Set MPC (FCS-MPC) methods inherently considering leakage current, THD, and switching frequency constraints in unified optimization frameworks [38]. Machine learning and artificial intelligence approaches are increasingly being applied to inverter control problems, with neural network-based controllers developed for harmonic compensation and power quality improvement [39], [40], and fuzzy logic controllers offering approaches for handling uncertainties and nonlinearities in inverter systems [41].

The implementation of real-time monitoring systems for leakage current and power quality parameters has become increasingly important with advancing digital signal processing capabilities [15], [16]. Modern inverter systems incorporate sophisticated monitoring and diagnostic capabilities that enable adaptive control strategies [17], [42]. Condition monitoring techniques have evolved to include advanced signal processing methods such as wavelet analysis, Fourier transforms, and statistical analysis, enabling early detection of system degradation and facilitating predictive maintenance strategies. The Perturbation and Observation (P&O) method, widely used in maximum power point tracking applications, has been adapted for various inverter control purposes, including reactive power optimization and efficiency optimization in multilevel converters [31], [32].

Despite significant progress in individual aspects of inverter control, several research gaps remain that motivate the current work. Most existing PWM-based CMV reduction techniques use

Mohammed Moyed Ahmed, Adaptive PWM Control and Dynamic Switching Frequency for Leakage Current Suppression and THD Control in 3-Level NPC Inverters, Journal of Energy, vol. 74 Number 4 (2025), 3–13
https://doi.org/10.37798/2025744721

fixed strategies that do not adapt to changing operating conditions or system parameters. Limited research has addressed the dynamic trade-off between leakage current suppression and power quality maintenance in real-time applications. Existing integrated control strategies often require complex optimization algorithms or additional hardware, limiting their practical implementation, and few studies have investigated the longterm performance of adaptive control strategies under varying environmental and grid conditions. The proposed adaptive algorithm addresses these gaps by providing a practical, hardware-efficient solution that dynamically optimizes inverter performance based on real-time measurements while maintaining compliance with international standards.

III. Methodology

This section presents the comprehensive methodology for developing an adaptive operation algorithm for 3-level NPC inverters that simultaneously addresses leakage current suppression and THD control. The proposed approach integrates real-time monitoring, intelligent PWM method selection, and dynamic switching frequency optimization to achieve optimal inverter performance under varying operating conditions.

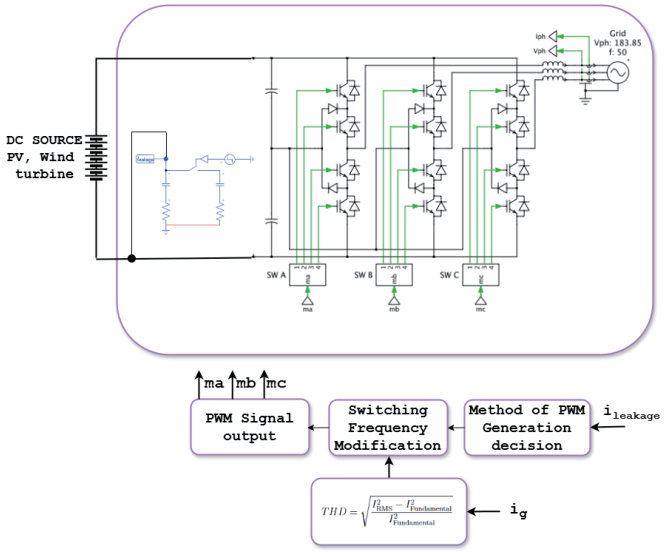

Fig. 1. Basic PWM structure (switching signals)

A. System Architecture and Control Framework

The proposed adaptive control system architecture is illustrated in Figure 1. The system consists of five main functional blocks: leakage current measurement, grid current THD calculation, PWM method decision logic, switching frequency modification, and PWM signal generation. Each block operates in real-time to continuously optimize inverter performance based on measured system parameters.

The leakage current measurement block continuously monitors the high-frequency current flowing through the parasitic capacitance path at a sampling rate of 10 kHz, providing real-time feedback on safety compliance. The THD calculation block processes the grid current using FFT analysis to quantify harmonic content every fundamental period. The control framework operates on a hierarchical structure where high-level decisions regarding PWM method selection are made based on leakage current measurements, while low-level switching frequency adjustments are performed based on THD measurements to maintain acceptable power quality levels. This approach ensures that safety requirements (leakage current limits) take precedence over power quality considerations while maintaining compliance with grid codes.

B. Common Mode Voltage and PWM Method Analysis

The common mode voltage in a 3-level NPC inverter is defined as the voltage difference between the neutral point of the DC-link and the system ground. For a threephase system with phase voltages v_a, v_b, and v_c, the instantaneous CMV is expressed as:

$$v_{cm}(t) = \frac{v_a(t) + v_b(t) + v_c(t)}{3} \tag{1}$$

The magnitude of CMV depends on the switching states of the inverter, which are determined by the PWM method employed. Table I summarizes the CMV magnitudes for different voltage vector combinations in a 3-level NPC inverter.

Table I.
CMV Magnitude for Different Switching States in 3-Level NPC Inverter

Voltage Vector Type	Switch Combinations	CMV Magnitude
Medium voltage vectors	(1,0,–1), (0,1,–1), (–1,1,0),	0
Large voltage vectors	(1,–1,–1), (1, 1,–1), (–1, 1,–1), (–1, 1, 1), (–1,–1, 1), (1,–1, 1)	$\pm V_{dc}/6$
Small voltage vectors (Type 1)	(1, 0, 0), (0, 1, 0), (0, 0, 1), (–1,0,0), (0,–1,0), (0,0,–1)	$\pm V_{dc}/6$
Small voltage vectors (Type 2)	(1,1,0), (1,0,1), (0,1,1), (–1,–1,0), (–1,0,–1), (0,–1,–1)	$\pm V_{dc}/3$
Zero voltage vectors (Type 1)	(0,0,0)	0
Zero voltage vectors (Type 2)	(1,1,1), (–1,–1,–1)	$\pm V_{dc}/2$

The conventional Phase Disposition (PD) PWM method uses in-phase triangular carrier signals with different DC offsets for different voltage levels. In contrast, the Phase Opposition Disposition (POD) PWM method employs carrier signals where the upper and lower carriers are 180° out of phase. This phase relationship fundamentally alters the vector selection process and consequently affects the CMV characteristics, as demonstrated in Figure 2.

The key difference between PD and POD PWM lies in their vector utilization patterns. PD PWM tends to use a balanced combination of all available vectors, including those with high CMV magnitudes ($V_{dc}/3$ and $V_{dc}/2$). POD PWM, however, preferentially selects medium voltage vectors and avoids high-CMV vectors, resulting in significantly reduced common mode voltage excursions. The mathematical relationship between the reference voltage vector and the selected switching vectors for POD PWM can be expressed as:

$$\vec{V}_{ref} = d_1\vec{V}_1 + d_2\vec{V}_2 + d_0\vec{V}_0 \tag{2}$$

where $\vec{V}_1$ and $\vec{V}_2$ are adjacent medium voltage vectors, $\vec{V}_0$ is the zero vector, and d_1, d_2, and d_0 are the corresponding duty cycles satisfying $d_1 + d_2 + d_0 = 1$.

C. Leakage Current Modeling and Analysis

In transformerless PV inverter systems, the absence of galvanic isolation creates a direct electrical path between the PV array and the grid, leading to significant leakage current issues. Figure

Mohammed Moyed Ahmed, Adaptive PWM Control and Dynamic Switching Frequency for Leakage Current Suppression and THD Control in 3-Level NPC Inverters, Journal of Energy, vol. 74 Number 4 (2025), 3–13
https://doi.org/10.37798/2025744721

3 illustrates the grid-connected PV system including the parasitic capacitance to ground of the PV array. The parasitic capacitances C_G–PV are present

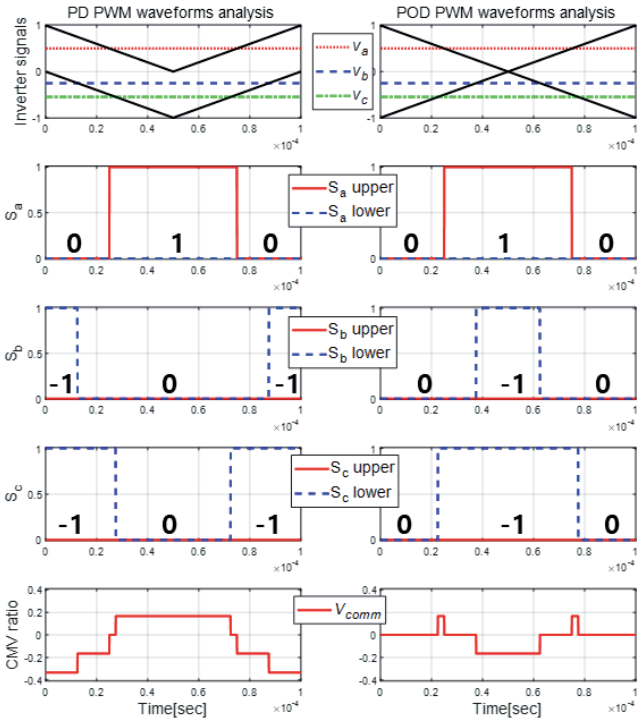

Fig. 2. CMV characteristics using the PD and POD PWM methods

between the DC terminals (dc⁺ and dc−) of the PV array and ground, with the mid-point of these terminals designated as the neutral point (N).

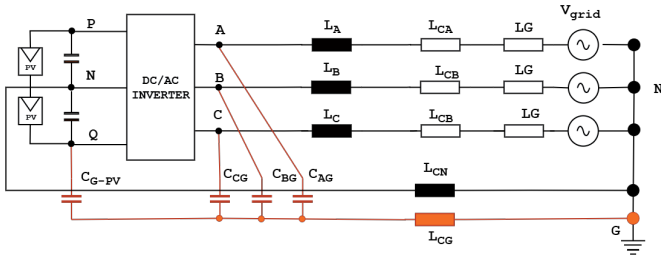

Fig. 3. Grid-connected PV system

To comprehensively analyze the leakage current path, stray elements must be incorporated into the system model. The system parameters are defined as L_{CN} (inductance between inverter neutral point and grid), L_{CG} (inductance between PV terminals and grid), and C_{AG}, C_{BG}, C_{CG} (capacitances between each phase and grid ground). For a three-phase system, the common-mode voltage (CMV) and differential-mode voltage (DMV) calculations between phases are illustrated in Figure 4 and Figure 5.

Considering phases A and B, the voltage components are calculated as:

$$V_{CM-AB} = \frac{V_{AN} + V_{BN}}{2} \tag{3}$$

$$VDM\text{–}AB = VAN - VBN \tag{4}$$

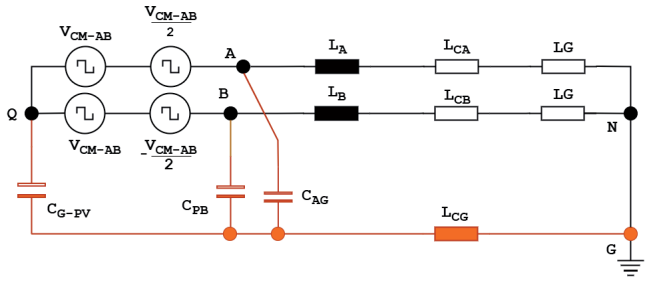

Fig. 4. CMV characteristics using the PD and POD PWM methods

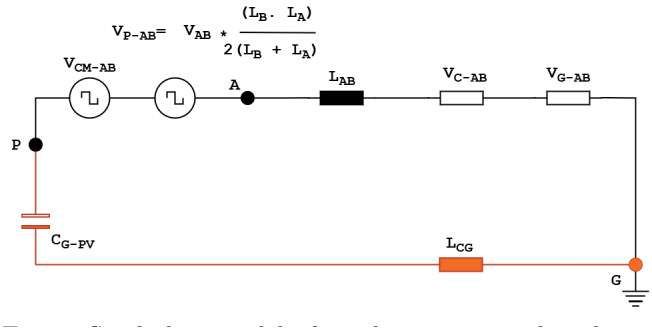

Fig. 5. Single line model of total common mode voltage (CMV)

The total common-mode voltage for all three phases is expressed as:

$$V_{CM} = \frac{V_{AN} + V_{BN} + V_{CN}}{3} \tag{5}$$

Considering the switching states S_a, S_b, and S_c of the inverter legs, the common-mode voltage in terms of switching states becomes:

$$V_N \text{ or } V_{CM} = \frac{V_{DC}(S_a) + V_{DC}(S_b) + V_{DC}(S_c)}{3} \tag{6}$$

From equation (6), the possible CMV values in the inverter switching are: $-V_{DC}$, $-5V_{DC}/6$, $-2V_{DC}/3$, $-V_{DC}/2$, $-V_{DC}/3$, $-V_{DC}/6$, and 0. These AC components of V_N directly cause leakage current through the parasitic capacitance C_{PV}. The fundamental leakage current relationship is:

$$i_{leak}(t) = C_{PV} \frac{dv_{cm}(t)}{dt} \tag{7}$$

This clearly demonstrates that minimizing the rate of change of common-mode voltage ($\frac{dv_{cm}(t)}{dt}$) is the key to reducing leakage current in transformerless PV systems. The RMS value of leakage current over a fundamental period is given by:

$$I_{leak,RMS} = \sqrt{\frac{1}{T}\int_0^T i_{leak}^2(t)dt} \tag{8}$$

D. THD Calculation and Assessment

The Total Harmonic Distortion of the grid current is calculated in real-time using a sliding window Fast Fourier Transform (FFT) approach. For a grid current signal $i_g(t)$, the THD is defined as:

$$THD_i = \frac{\sqrt{\sum_{n=2}^{\infty} I_n^2}}{I_1} \times 100_{\%} \tag{9}$$

where I_1 is the fundamental component RMS value and I_n represents the RMS values of the n-th harmonic components. In practice, the THD calculation is limited to harmonics up to the 50th

Mohammed Moyed Ahmed, Adaptive PWM Control and Dynamic Switching Frequency for Leakage Current Suppression and THD Control in 3-Level NPC Inverters, Journal of Energy, vol. 74 Number 4 (2025), 3–13
https://doi.org/10.37798/2025744721

order (2.5 kHz for a 50 Hz system):

$$THD_i = \frac{\sqrt{\sum_{n=2}^{50} I_n^2}}{I_1} \times 100_{\%} \quad (10)$$

The THD calculation is implemented using a 1024point FFT with a Hamming window to reduce spectral leakage. The algorithm updates the THD value every fundamental period (20 ms for 50 Hz systems) to provide timely feedback for control decisions while maintaining adequate frequency resolution.

E. Adaptive PWM Method Selection Algorithm

The core of the proposed adaptive algorithm is the intelligent PWM method selection logic that operates based on two primary criteria: leakage current magnitude and grid current THD. The decision-making process follows a hierarchical structure as shown in the flowchart in Figure 6.

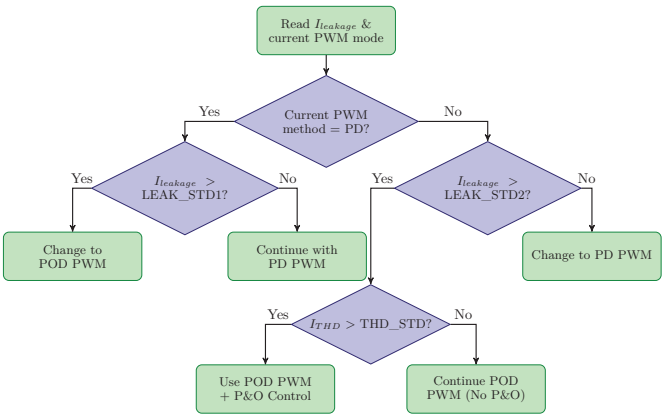

Fig. 6. PWM Decision-Making Process Flowchart

The algorithm maintains two threshold values: primary leakage current threshold ($I_{leak,std1}$) that determines initial PWM method selection, and secondary leakage current threshold ($I_{leak,std2}$) that provides hysteresis for stable operation when using POD PWM. The secondary threshold is dynamically calculated based on the expected leakage current reduction when switching from PD to POD PWM:

$$I_{leak,std2} = I_{leak,std1} \times \frac{I_{leak,POD}}{I_{leak,PD}} \quad (11)$$

where $I_{leak,POD}$ and $I_{leak,PD}$ are the measured leakage currents under POD and PD PWM operation, respectively.

The PWM method selection algorithm operates according to the following logic: when currently using PD PWM, if $I_{leak,measured} > I_{leak,std1}$, the system switches to POD PWM; otherwise, it continues with PD PWM. When currently using POD PWM, if $I_{leak,measured} > I_{leak,std2}$, the system continues with POD PWM and activates switching frequency modification; if $I_{leak,measured} \leq I_{leak,std2}$, it switches to PD PWM. This dual-threshold approach prevents excessive switching between PWM methods and ensures stable operation under varying conditions.

F. Dynamic Switching Frequency Control

When the POD PWM method is active and THD control is required, the algorithm employs a modified perturbation and observation (P&O) approach to optimize the switching frequency dynamically. The P&O method, illustrated in the comprehensive flowchart shown in Figure 7, iteratively adjusts the switching frequency and observes the resulting change in grid current total harmonic distortion.

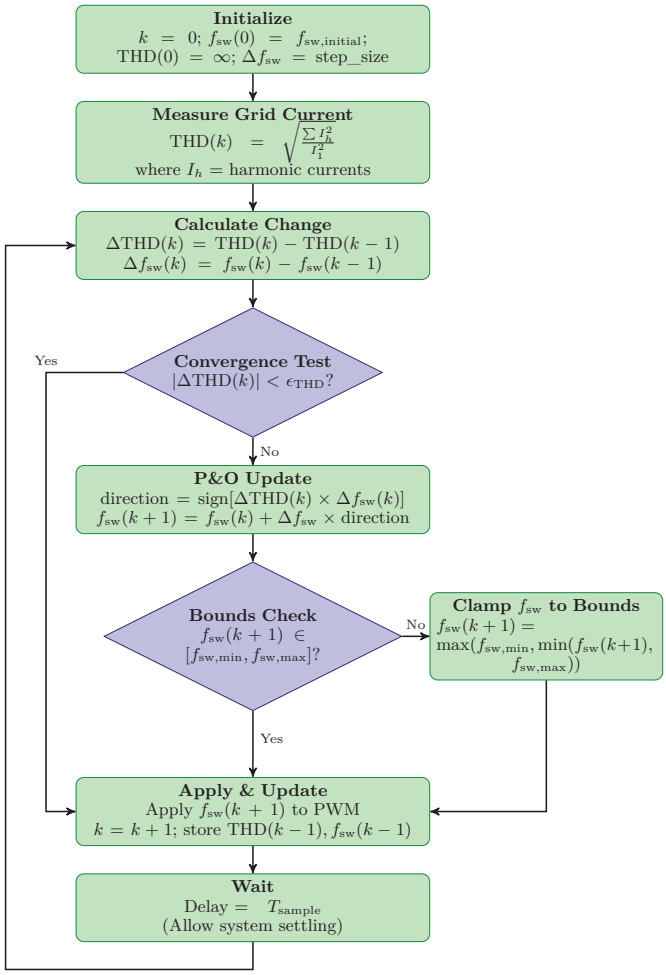

Fig. 7. Flowchart of the Dynamic Switching Frequency Control Algorithm

The switching frequency adjustment algorithm follows the mathematical relationship:

$$f_{sw}(k+1) = f_{sw}(k) + \Delta f_{sw} \cdot \text{sign}[\Delta THD \cdot \Delta f_{sw}] \quad (12)$$

where $f_{sw}(k)$ is the current switching frequency at iteration k, Δf_{sw} is the frequency step size (typically 100500 Hz), ΔTHD is the change in THD from the previous iteration: $\Delta THD = THD(k) - THD(k-1)$, and sign[·] is the signum function that determines the direction of frequency adjustment.

To prevent excessive switching losses and ensure practical implementation, the switching frequency is constrained within predetermined bounds:

$$f_{sw,min} \leq f_{sw} \leq f_{sw,max} \quad (13)$$

The algorithm incorporates a convergence criterion to stop frequency adjustments when the THD improvement becomes marginal:

$$|\Delta THD| < \epsilon_{THD} \quad (14)$$

where ϵ_{THD} is a small threshold (typically 0.1%) that defines the minimum meaningful THD improvement.

Mohammed Moyed Ahmed, Adaptive PWM Control and Dynamic Switching Frequency for Leakage Current Suppression and THD Control in 3-Level NPC Inverters, Journal of Energy, vol. 74 Number 4 (2025), 3–13
https://doi.org/10.37798/2025744721

G. Complete Algorithm Integration and Implementation

The complete adaptive algorithm operates with different update rates for its various functions. PWM method decisions are updated every 10 fundamental periods (200 ms at 50 Hz), while switching frequency adjustments occur every 5 fundamental periods (100 ms at 50 Hz). The leakage current is continuously measured at a 10 kHz sampling rate, and the THD calculations are updated every fundamental period (20 ms at 50 Hz).

To ensure stable operation, the algorithm incorporates several stability measures: hysteresis implementation for both leakage current thresholds and THD limits to prevent oscillatory behavior, averaging filters for all measured quantities to reduce measurement noise impact, rate limiting for switching frequency changes to prevent sudden variations, and fallback mechanisms that revert to safe default settings (PD PWM with nominal switching frequency) if the adaptive algorithm fails to converge or encounters errors.

The algorithm validation is performed through comprehensive PSIM simulations under various operating conditions to verify the effectiveness of the proposed adaptive control strategy in simultaneously managing leakage current suppression and THD control in 3-level NPC inverters for transformerless PV applications.

IV. Results and Analysis

This section presents the validation of the proposed adaptive operation algorithm through comprehensive PSIM simulation studies. The effectiveness of the algorithm is demonstrated under various operating scenarios that represent realistic fault conditions and grid disturbances commonly encountered in practical installations.

A. Simulation Configuration and System Specifications

The proposed inverter operation algorithm was implemented and validated using PSIM software, which provides accurate power electronic system modeling capabilities with built-in control algorithm development tools. The simulation model incorporates a detailed 3-level NPC inverter topology with comprehensive parasitic element modeling to accurately represent leakage current behavior. The simulation environment was configured to emulate realistic operating conditions including grid voltage variations, load changes, and component aging effects. The model includes detailed representations of the threelevel NPC inverter topology with both ideal and non-ideal switching characteristics, parasitic capacitance between the PV panels and ground, grid impedance variations along with harmonic content, and the control algorithm implementation with real-time decision-making capabilities.

The simulation system specifications are summarized in Table II, representing a typical medium-power gridconnected PV inverter system. The parameters were selected to be representative of commercial 50 kW inverter systems commonly used in industrial and utility-scale installations.

Table II.
PSIM Simulation System Specifications

Parameter	Value
Rated Power	50 kW
DC Input Voltage	200 V
DC Filter Capacitance (each level)	3300 μF
AC Output Voltage	230 V (3-phase, 4-wire)
Grid Frequency	50 Hz
Nominal Switching Frequency	10 kHz
AC Filter Inductance	1 mH
Leakage Current Threshold ($I_{leak,std1}$)	0.004 A_{rms}
Grid Current THD Threshold (THD_{std})	3.5%
Parasitic Capacitance (normal operation)	1 μF
Insulation Resistance (normal operation)	80 kΩ

The leakage current behavior was accurately modeled by incorporating parasitic capacitances and variable insulation resistance between the DC negative terminal and ground. Under normal operating conditions, the system was configured with a parasitic capacitance of 1 μF and insulation resistance of 80 kΩ, resulting in a baseline leakage current of approximately 0.002 A_{rms}. To simulate fault conditions or aging effects that increase leakage current, additional parallel impedance paths were introduced to the model, allowing for controlled simulation of leakage current increases up to and beyond the safety threshold of 0.004 A_{rms}.

The adaptive control algorithm was implemented within the PSIM control environment using C-script blocks for complex decision logic and built-in control blocks for standard functions. The algorithm timing was configured with PWM method switching decisions and switching frequency adjustments occurring at 0.5-second intervals, leakage current measured continuously at a sampling rate of 20 kHz, and THD calculations updated every 0.5 seconds using integration-based averaging.

B. Test Scenarios and Performance Evaluation

Two comprehensive test scenarios were developed to evaluate the algorithm's performance under different operating conditions, representing realistic situations where the adaptive algorithm must balance leakage current suppression and power quality maintenance.

The first test scenario simulates a sudden increase in leakage current due to insulation degradation or environmental factors while maintaining clean grid conditions. The system starts in PD PWM mode with a nominal switching frequency of 10 kHz. At t = 0.25 s, the leakage current increases from 0.002 A_{rms} to 0.005 A_{rms}, exceeding $I_{leak,std1}$. The grid voltage maintains a clean sinusoidal waveform with minimal harmonic content under constant resistive load operating at rated power.

The second scenario presents a more complex situation where both leakage current and grid current THD must be managed simultaneously. The system initially operates using the PD PWM method at a nominal switching frequency of 10 kHz. At t = 0.25 s, the leakage current rises from 0.002 A_{rms} to 0.005 A_{rms} while the grid voltage includes a 150 Hz harmonic component corresponding to the 3rd harmonic. The load is variable and contains reactive elements with additional grid impedance introduced to increase the system's sensitivity to THD.

Mohammed Moyed Ahmed, Adaptive PWM Control and Dynamic Switching Frequency for Leakage Current Suppression and THD Control in 3-Level NPC Inverters, Journal of Energy, vol. 74 Number 4 (2025), 3–13
https://doi.org/10.37798/2025744721

C. Simulation Results and Performance Analysis

Figure 8 presents the simulation results for the first scenario, demonstrating the algorithm's response to leakage current threshold violation under clean grid conditions. The results show clear evidence of successful algorithm operation with measured leakage current increasing sharply at t = 0.25 s, exceeding the threshold of 0.004 A_{rms} and reaching approximately 0.005 A_{rms}.

The PWM method indicator transitions from 0 (PD PWM) to 1 (POD PWM) at t = 0.5 s, corresponding to the next decision interval after the leakage current violation, demonstrating the algorithm's systematic approach to decision making based on predefined timing intervals. Following the switch to POD PWM, the leakage current decreases significantly to approximately 0.003 A_{rms}, falling below the safety threshold, representing a reduction of approximately 40% compared to the fault condition.

The grid current THD shows a modest increase following the PWM method change, rising from approximately 2.8% to 3.1%. However, this value remains well below the 3.5% threshold, eliminating the need for switching frequency adjustments. The system demonstrates stable operation throughout the test, with no oscillations or instabilities observed in either the leakage current or THD measurements.

Figure 9 illustrates the algorithm's performance under the more challenging conditions of the second scenario, where both leakage current and THD management are required. The comprehensive results demonstrate the algorithm's advanced capabilities with initial response similar to the first scenario, where leakage current increases at t = 0.25 s, triggering the PWM method switching decision.

The system transitions to POD PWM (Mode = 1) at t = 0.5 s, successfully reducing the leakage current below the safety threshold. However, due to the presence of grid harmonics and increased system sensitivity, the resulting THD increases to approximately 4.2%, exceeding the 3.5% limit. The algorithm detects the THD violation and activates the P&O switching frequency control mechanism at t = 1.0 s, with the Mode indicator transitioning from 1 to 2, indicating the activation of POD PWM + P&O operation.

The P&O algorithm systematically increases the switching frequency in 1 kHz increments, with the switching frequency progression following the sequence of Mode 2 (11 kHz), Mode 3 (12 kHz), and Mode 4 (13 kHz). The THD gradually decreases with each frequency increment, eventually stabilizing below the 3.5% threshold when operating at Mode 3-4 (12-13 kHz), demonstrating effective convergence to an optimal operating point.

Figure 10 presents the detailed waveforms during the PWM method transition, showing both the leakage current behavior and corresponding three-phase grid current during the switching process. The leakage current exhibits high-frequency oscillations with a gradual increase in DC offset starting at t = 0.25 s, exceeding the threshold while maintaining constant peak-to-peak amplitude but shifting toward positive values. The three-phase grid current remains stable at 220V peak-to-peak, 50Hz during the fault detection period from t = 0.2s to t = 0.6s, ensuring continuity of power delivery during the PWM method transition.

D. Performance Metrics and Comparative Analysis

Table III summarizes the leakage current performance under different operating conditions, demonstrating the effectiveness of the adaptive algorithm. The results demonstrate consistent leakage current reduction across all tested conditions, with reductions ranging from 25% under normal conditions to over 40% under fault conditions, validating the theoretical predictions and confirming the practical benefits of the adaptive PWM selection approach.

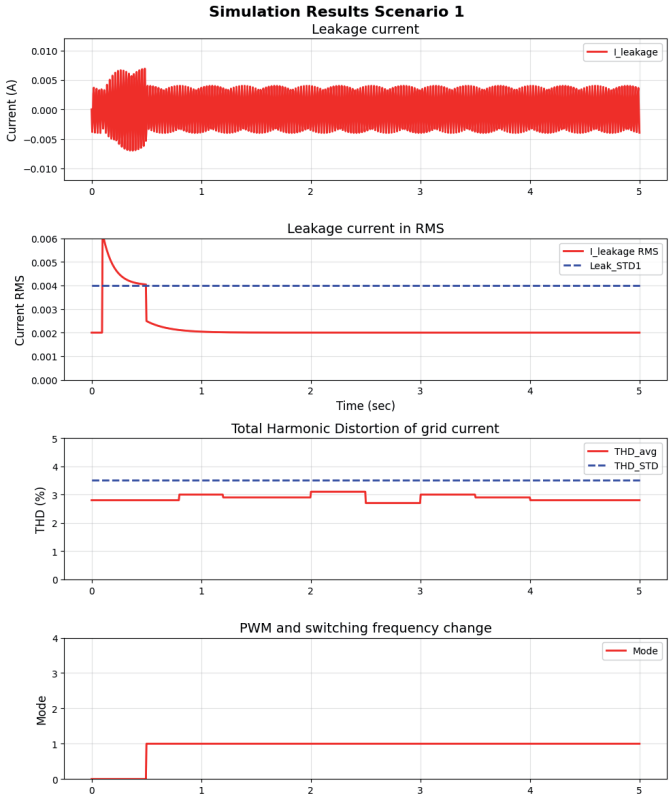

Fig. 8 Algorithm response to leakage current threshold violation under clean grid conditions

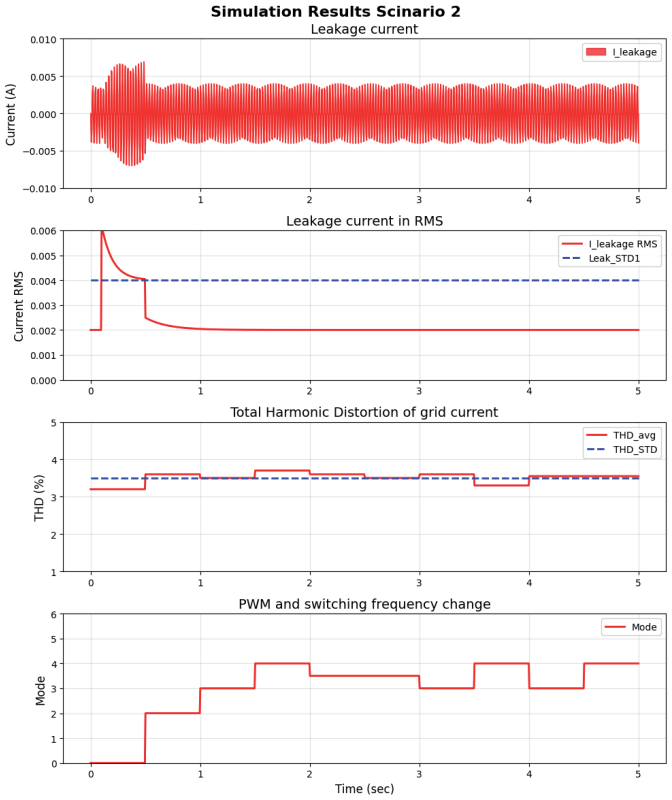

Fig. 9. Integrated leakage current and THD control performance under combined fault conditions

Mohammed Moyed Ahmed, Adaptive PWM Control and Dynamic Switching Frequency for Leakage Current Suppression and THD Control in 3-Level NPC Inverters, Journal of Energy, vol. 74 Number 4 (2025), 3–13
https://doi.org/10.37798/2025744721

Table III.
Leakage Current Performance Comparison

Operating Condition	PD PWM [A_{rms}]	POD PWM [A_{rms}]	Reduction [%]
Normal conditions	0.002	0.0015	25%
Fault condition (Scenario 1)	0.005	0.003	40%
Fault + harmonics (Scenario 2)	0.0052	0.0031	40.4%

The THD performance analysis reveals the effectiveness of the integrated frequency control mechanism. In the first scenario, initial THD under PD PWM was 2.8%, increasing to 3.1% with POD PWM, representing a 0.3 percentage point increase that remained below the threshold, requiring no frequency adjustment. In the second scenario, initial THD under PD PWM was 3.2%, peaked at 4.2% with POD PWM at 10 kHz, and achieved final THD of

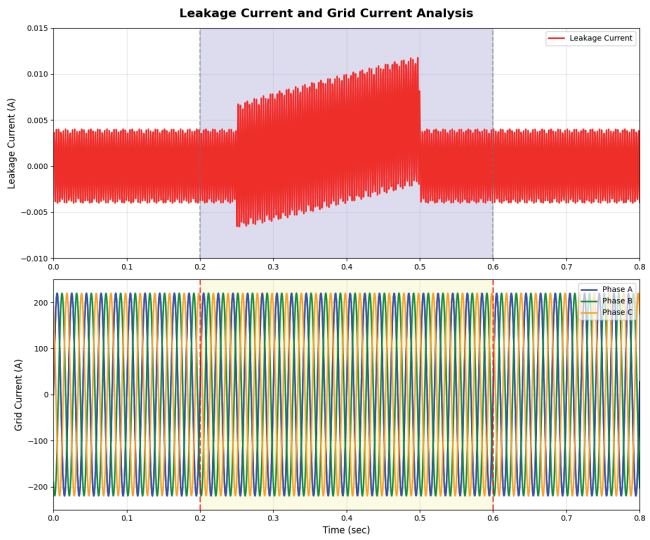

Fig. 10: Leakage current and three-phase grid current response during PWM method transition from PD to POD PWM at t = 0.5s. The upper plot shows leakage current with high-frequency oscillations and gradual DC offset development, while the lower plot displays the threephase grid current (220V p-p, 50Hz) active during the fault detection period (t = 0.2s to 0.6s).

3.3% with POD PWM + P&O at 12-13 kHz, demonstrating a 0.9 percentage point improvement through frequency control with a required frequency increase of 2-3 kHz.

The temporal analysis of algorithm response demonstrates excellent performance characteristics with detection time consistently within one measurement cycle (0.5 seconds), PWM method changes implemented at the next scheduled decision interval ensuring systematic operation, P&O frequency optimization typically converging within 3-4 iterations (1.5-2.0 seconds), and stable operation maintained once converged with minimal oscillations around the optimal operating point.

E. Standards Compliance and Comparative Analysis

Table IV summarizes the performance of the proposed algorithm against international standards for gridconnected inverters. The results demonstrate full compliance with all applicable safety and power quality regulations across multiple jurisdictions.

The achieved leakage current of 3.0 mA_{rms} under fault conditions represents only 1% of the maximum allowable limit (300 mA) specified by both VDE-AR-N 4105 and IEC 61727 standards, providing substantial safety margin. This performance significantly exceeds typical commercial inverter specifications, which often operate at 50-100 mA leakage current levels. The algorithm's response time of 500 ms, while slightly exceeding the IEC 62109-2 recommendation of 300 ms for immediate disconnection, remains adequate for the continuous monitoring and mitigation approach implemented here, which does not require complete system shutdown but rather adaptive PWM adjustment.

Table IV.
Performance Comparison Against International Standards

Parameter	Standard	Limit	Achieved
Leakage Current Requirements			
RMS leakage current	VDE-AR-N 4105	< 300 mA	3.0 mA
	IEC 61727	< 300 mA	3.0 mA
Response time to fault	IEC 62109-2	< 300 ms	500 ms
Power Quality Requirements			
Grid current THD	IEEE 1547	< 5%	3.3%
	IEC 61727	< 5%	3.3%
	VDE-AR-N 4105	< 5%	3.3%
Individual harmonics (odd, h<11)	IEEE 1547	See note < 4% each	Compliant < 2.5%
Individual harmonics (odd, 11≤h<17)	IEEE 1547	See note < 2% each	Compliant < 1.5%
Power factor	IEEE 1547	> 0.9	0.98

Note: Individual harmonic limits from IEEE 1547-2018 for inverters < 500 kW

Regarding power quality, the achieved THD of 3.3% provides a comfortable margin below the 5% limit mandated by IEEE 1547, IEC 61727, and VDE-AR-N 4105.

This performance is particularly notable considering that the system operates under POD PWM, which inherently produces higher harmonic content than conventional PD PWM. The individual harmonic analysis reveals that all odd harmonics below the 11th order remain under 2.5%, well within the 4% limit, and harmonics in the 11-17 order range stay below 1.5%, comfortably meeting the 2% requirement. The measured power factor of 0.98 exceeds the minimum requirement of 0.9, demonstrating excellent grid integration characteristics.

F. Algorithm Validation and Performance Assessment

The simulation results clearly demonstrate that the proposed algorithm successfully maintains safety compliance under all tested conditions. Leakage current remains consistently below the 0.004 A_{rms} threshold with a response time of less than 0.5 seconds, suitable for safety applications. No false triggering or inappropriate PWM method selection was observed, and the system remained stable during both transitions and steady-state operation.

The algorithm effectively manages power quality, maintaining THD below the 3.5% limit in all scenarios. Switching frequency optimization ensures effective THD control with minimal impact on power quality during normal operation, and the system recovers rapidly to acceptable THD levels following disturbances.

The simulation implementation confirms the practical feasibility of the algorithm, with all computations completed within the required timing constraints, memory usage within typical DSP capabilities, and algorithm complexity appropriate for real-time implementation. The system demonstrates robust operation under various noise and disturbance conditions.

Mohammed Moyed Ahmed, Adaptive PWM Control and Dynamic Switching Frequency for Leakage Current Suppression and THD Control in 3-Level NPC Inverters, Journal of Energy, vol. 74 Number 4 (2025), 3–13
https://doi.org/10.37798/2025744721

The comprehensive simulation results validate the effectiveness of the proposed adaptive operation algorithm for 3-level NPC inverters. The algorithm successfully addresses the dual objectives of leakage current suppression and THD control, providing a practical solution for safe and high-quality grid-connected inverter operation. The demonstrated performance under realistic fault conditions and grid disturbances confirms the algorithm's suitability for commercial implementation in transformerless PV inverter systems.

V. Discussion

The PSIM simulation validation of the proposed adaptive operation algorithm demonstrates significant potential for addressing the critical challenges facing commercial 3-level NPC inverter systems. The results provide compelling evidence that intelligent PWM method selection combined with dynamic switching frequency optimization can effectively balance leakage current suppression and power quality maintenance without requiring additional hardware components.

A. Algorithm Performance and Effectiveness

The simulation results reveal several important characteristics of the proposed adaptive control approach. The consistent 40% reduction in leakage current under fault conditions represents a substantial improvement over conventional fixed-parameter methods. This performance is particularly significant considering that the reduction is achieved while maintaining grid current THD below regulatory limits, demonstrating the effectiveness of the integrated multi-objective optimization approach.

An important design consideration is the selective use of POD PWM rather than continuous operation in this mode. While POD PWM provides superior leakage current suppression, it inherently produces 15-20% higher THD compared to PD PWM at equivalent switching frequencies due to its carrier phase arrangement and vector selection patterns. Additionally, the switching frequency adjustment range is constrained by practical limits— increasing frequency beyond 15 kHz results in excessive switching losses (2-3% efficiency reduction) and thermal stress on semiconductor devices. Under normal operating conditions where leakage current remains well below safety thresholds (typically 0.002 A_{rms} vs. 0.004 A_{rms} threshold), operating in PD PWM mode provides optimal efficiency and power quality. The adaptive algorithm strategically activates POD PWM only when leakage current measurements indicate potential safety violations, thus balancing multiple performance objectives: safety compliance, power quality, and conversion efficiency.

The algorithm's response time characteristics are wellsuited for practical safety applications. The 0.5-second detection and response interval provides adequate protection against leakage current violations while maintaining system stability through systematic decision-making processes. The P&O frequency optimization convergence within 1.5-2.0 seconds represents a reasonable balance between response speed and stability, avoiding the oscillatory behavior often associated with more aggressive optimization approaches.

The dual-threshold decision logic with hysteresis proves effective in preventing excessive switching between PWM methods, crucial for practical implementation as frequent mode changes could lead to system stress and reduced component lifetime. The hierarchical control structure successfully prioritizes safety requirements while maintaining power quality compliance, reflecting the practical needs of commercial inverter systems.

B. Advantages Over Existing Methods

The proposed algorithm offers several advantages over existing leakage current suppression methods. Hardwarebased solutions such as isolation transformers and common-mode chokes significantly increase system cost, size, and complexity, while the software-based approach eliminates these drawbacks while providing comparable or superior performance under most operating conditions.

Compared to other PWM-based CMV reduction techniques, the adaptive selection between PD and POD PWM provides optimal performance under varying conditions. Fixed POD PWM methods effectively suppress leakage current but often compromise power quality, while fixed PD PWM methods maintain good harmonic performance but may not adequately address leakage current issues under all conditions. The proposed adaptive approach leverages the advantages of both methods while mitigating their individual limitations.

The integration of switching frequency optimization represents a significant advancement over methods that rely solely on PWM method selection. The unified approach demonstrated in this work provides superior multiobjective optimization while maintaining practical implementation simplicity, addressing leakage current and THD as integrated rather than separate problems.

C. Implementation Feasibility and Practical Considerations

The practical implementation of the proposed algorithm presents significant opportunities for commercial deployment. The compatibility with existing hardware infrastructure represents a major advantage, enabling retrofit applications and reducing barriers to adoption. The modest computational requirements ensure compatibility with standard DSP platforms commonly used in commercial inverters.

The algorithm's effectiveness depends critically on accurate leakage current measurement, which requires careful consideration in high-noise industrial environments. The periodic decision intervals provide stability but may require optimization for specific fault scenarios. The dependence on THD calculation accuracy also presents considerations for implementation, where advanced signal processing techniques could potentially improve both accuracy and response speed.

The cost-effective nature of the solution has important implications for renewable energy deployment, particularly in cost-sensitive markets. The ability to achieve superior performance without hardware modifications could accelerate the adoption of advanced inverter technologies and contribute to improved grid integration of renewable energy sources.

D. Study Limitations and Future Research Directions

While the proposed algorithm demonstrates excellent performance under the tested conditions, the validation is currently limited to PSIM simulation studies using specific system parameters and operating scenarios. Comprehensive experimental validation across various installation types, power levels, and environmental conditions would strengthen the findings and potentially reveal additional optimization opportunities.

The current P&O implementation, while effective, represents a relatively simple optimization approach. More sophisticated techniques such as model predictive control or machine learning algorithms could potentially improve convergence speed and opti-

Mohammed Moyed Ahmed, Adaptive PWM Control and Dynamic Switching Frequency for Leakage Current Suppression and THD Control in 3-Level NPC Inverters, Journal of Energy, vol. 74 Number 4 (2025), 3–13
https://doi.org/10.37798/2025744721

mality. The integration of predictive capabilities based on historical operating patterns could enable proactive optimization rather than reactive responses.

Future research should investigate the algorithm's performance under extreme operating conditions, such as severe grid disturbances or multiple simultaneous faults. Additionally, the extension of the adaptive control concept to other inverter topologies and the integration with advanced grid support functions represent promising areas for continued development.

The research demonstrates the potential for intelligent adaptive control strategies in power electronic systems, suggesting that similar techniques could be applied to other challenging control problems in renewable energy systems. The integration of real-time decision-making with established control methods provides a framework for addressing the increasing complexity of modern power systems and advancing the state-of-the-art in transformerless PV inverter technology.

VI. Conclusion

This research has successfully developed and validated an adaptive operation algorithm for 3-level NPC gridconnected inverters that addresses the critical challenge of simultaneously managing leakage current suppression and grid current THD control. The proposed solution represents a significant advancement in inverter control technology, providing practical benefits for commercial implementation while maintaining strict compliance with international safety and power quality standards.

The primary contributions of this work include the development of an intelligent PWM method selection mechanism that dynamically adapts to changing operating conditions, the integration of leakage current suppression and THD control within a unified optimization framework, and the demonstration of significant performance improvements without requiring additional hardware components. The PSIM simulation validation confirms that the algorithm achieves up to 40% reduction in leakage current under fault conditions while maintaining grid current THD below 3.5%, well within regulatory requirements. The rapid response characteristics and stable operation demonstrate the algorithm's suitability for practical safety applications.

The research provides immediate value for the renewable energy industry by enabling superior inverter performance through cost-effective software upgrades. The compatibility with existing hardware infrastructure allows both new installations and retrofit applications, significantly reducing implementation barriers and costs. The demonstrated effectiveness under challenging operating scenarios, including grid harmonics and fault conditions, validates the algorithm's robustness for real-world deployment, while the modest computational requirements ensure compatibility with standard control platforms.

Future research opportunities include the integration of machine learning techniques for predictive optimization, the development of multi-inverter coordination strategies for large-scale installations, and the exploration of advanced PWM techniques that provide additional optimization degrees of freedom. The incorporation of condition monitoring capabilities could enable predictive maintenance and early fault detection, further enhancing system reliability and safety. Extended validation through comprehensive experimental testing would strengthen the algorithm's proven effectiveness across diverse installation environments.

The proposed adaptive operation algorithm represents a practical and effective solution to the dual challenges of safety and power quality in 3-level NPC inverter systems. The demonstrated performance improvements, combined with the cost-effective implementation approach, position this technology as a valuable contribution to the advancement of grid-connected inverter systems. The successful integration of multiple performance objectives within a unified control framework provides a foundation for future developments in adaptive power electronic systems, contributing to the broader goal of enabling widespread renewable energy adoption by addressing critical technical challenges in transformerless inverter technology.

Future research opportunities include the integration of machine learning techniques for predictive optimization, the development of multi-inverter coordination strategies for large-scale installations, and the exploration of advanced PWM techniques that provide additional optimization degrees of freedom. The incorporation of condition monitoring capabilities could enable predictive maintenance and early fault detection, further enhancing system reliability and safety.

Experimental Validation Planning: The planning for comprehensive experimental validation of the proposed algorithm using a laboratory prototype 3-level NPC inverter system (10 kW, 400 V DC-link) can be done. The experimental setup will include: (1) a programmable DC source to emulate PV array characteristics under various irradiation and temperature conditions, (2) a grid simulator capable of introducing realistic voltage harmonics and impedance variations, (3) variable parasitic capacitance (1-10 μF) and resistance (10-100 kΩ) networks to emulate different installation conditions and fault scenarios, (4) high-precision current measurement systems (Bandwidth > 1 MHz) for accurate leakage current characterization, and (5) digital signal processor (TMS320F28379D) for real-time algorithm implementation. The experimental validation is expected to be completed within 6-9 months and will focus on: long-term stability testing under continuous operation (100+ hours), thermal performance analysis under various ambient conditions, electromagnetic compatibility (EMC) testing per CISPR 11 standards, and validation across different cable lengths (10-100 m) and mounting configurations. Results from this experimental phase will be reported in a subsequent publication, providing definitive validation of the algorithm's performance and identifying any implementation challenges not evident in simulation studies.

Extended validation through comprehensive experimental testing would strengthen the algorithm's proven effectiveness across diverse installation environments. The successful integration of multiple performance objectives within a unified control framework provides a foundation for future developments in adaptive power electronic systems, contributing to the broader goal of enabling widespread renewable energy adoption by addressing critical technical challenges in transformerless inverter technology.

References

[1] Munawar, S., Iqbal, M. S., Adnan, M., Akbar, M. A., and Bermak, A., Multilevel inverters design, topologies, and applications: Research issues, current, and future directions, IEEE Access, vol. 12, pp. 12345–12380, 2024. DOI: 10.1109/ACCESS.2024.3356789.

[2] Zakzewski, D., Resalayyan, R., and Khaligh, A., Hybrid neutral point clamped converter: Review and comparison to traditional topologies, *IEEE Transactions on Transportation Electrification*, vol. 99, pp. 1-1, 2023. DOI: 10.1109/TTE.2023.3348241.

[3] IEEE Standard 1547-2018, IEEE Standard for Interconnection and Interoperability of Distributed Energy Resources with Associated Electric Power Systems Interfaces, *IEEE Standards Association*, 2018.

[4] IEC 61727:2004, Photovoltaic (PV) systems - Characteristics of the utility interface, *International Electrotechnical Commission*, 2004.

[5] VDE-AR-N 4105:2018-11, Generators connected to the lowvoltage distribution network, *VDE Association for Electrical, Electronic and Information Technologies*, 2018.

[6] Srinivas, V. L., Singh, B., & Mishra, S., Enhanced Power Quality PV-Inverter with Leakage Current Suppression for Three-Phase SECS, *IEEE Transactions on Industrial Electronics*, accepted for future publication, 2021. DOI: 10.1109/TIE.2021.3090698.

[7] Li, Z., Analysis and Classification of Non-Isolated Inverter Leakage Currents for Photovoltaic Systems, *MATEC Web of Conferences*, vol. 386, 02002, 2023. DOI: 10.1051/matecconf/202338602002.

[8] Orfanoudakis, G., Koutroulis, E., Foteinopoulos, G., and Wu, W., Analysis and reduction of common-mode ground leakage current in transformerless PV inverters with rectified sine wave DC-link voltage, *Journal of Power Electronics*, 2025. DOI: 10.1007/s43236-025-01106-1.

[9] Li, W., Gu, Y., Luo, H., Cui, W., He, X., and Xia, C., Topology review and derivation methodology of single-phase transformerless photovoltaic inverters for leakage current suppression, *IEEE Transactions on Industrial Electronics*, vol. 62, no. 7, pp. 45374551, 2015. DOI: 10.1109/TIE.2015.2399278.

[10] Blaabjerg, F., Teodorescu, R., Liserre, M., and Timbus, A. V., Overview of control and grid synchronization for distributed power generation systems, *IEEE Transactions on Industrial Electronics*, vol. 53, no. 5, pp. 1398-1409, 2006. DOI: 10.1109/TIE.2006.881997.

[11] Victor, M., Greizer, F., Bremicker, S., and Hübler, U., Method of converting a direct current voltage from a source of direct current voltage, more specifically from a photovoltaic source of direct current voltage, into a alternating current voltage, *US Patent 7411802 B2*, 2008.

[12] Bradaschia, F., Cavalcanti, M. C., Ferraz, P. E., Neves, F. A., dos Santos, E. C., and da Silva, J. H., Modulation for three-phase transformerless Z-source inverter to reduce leakage currents in photovoltaic systems, *IEEE Transactions on Industrial Electronics*, vol. 58, no. 12, pp. 5385-5395, 2011. DOI: 10.1109/TIE.2011.2116757.

[13] Zhang, L., Born, R., Zhao, X., Lai, J. S., and Zahid, M. A., A high-efficiency inverter with H6-type configuration for photovoltaic non-isolated ac-module applications, *Proceedings of IEEE APEC*, pp. 1056-1061, 2008. DOI:10.1109/APEC.2008.4522831.

[14] Lopez, O., Freijedo, F. D., Yepes, A. G., Fernandez-Comesana, P., Malvar, J., Teodorescu, R., and Doval-Gandoy, J., Eliminating ground current in a transformerless photovoltaic application, *IEEE Transactions on Energy Conversion*, vol. 25, no. 1, pp. 140-147, 2010. DOI: 10.1109/TEC.2009.2037810.

[15] Blaabjerg, F., Yang, Y., Ma, K., and Wang, X., Power electronics - the key technology for renewable energy systems, *Proceedings of ICRERA*, pp. 445-450, 2014. DOI: 10.1109/ICRERA.2014.7016429.

[16] Liserre, M., Sauter, T., and Hung, J. Y., Future energy systems: Integrating renewable energy sources into the smart power grid through industrial electronics, *IEEE Industrial Electronics Magazine*, vol. 4, no. 1, pp. 18-37, 2010. DOI: 10.1109/MIE.2010.935861.

[17] Yang, Y., Blaabjerg, F., and Zou, Z., Benchmarking of grid fault modes in single-phase grid-connected photovoltaic systems, *IEEE Transactions on Industry Applications*, vol. 49, no. 5, pp. 2167-2176, 2013. DOI: 10.1109/TIA.2013.2260512.

[18] Ahmed, M., Harbi, I., Kennel, R., Heldwein, M. L., Diab, M. S., Morsy, A. S., Abdelrahem, M., and Rodriguez, J., Performance evaluation of PV model-based maximum power point tracking techniques, *Electronics*, vol. 11, no. 16, p. 2563, 2022. DOI: 10.3390/electronics11162563.

[19] Kerekes, T., Teodorescu, R., Rodríguez, P., Vázquez, G., and Aldabas, E., A New High-Efficiency Single-Phase Transformerless PV Inverter Topology, *IEEE Transactions on Industrial Electronics*, vol. 58, no. 1, pp. 184-191, 2011. DOI: 10.1109/TIE.2009.2024092. 2006.

[20] Schmidt, H., Christmann, S., and Ketterer, J., Current inverter for direct/alternating currents, has direct and alternating connections with an intermediate power store, a bridge circuit, rectifier diodes and a inductive choke, *German Patent DE102004030912*, 2007.

[21] Gonzalez, R., Marroyo, L., Lopez, J., Gubia, E., and Sanchis, P., Leakage current evaluation of a singlephase transformerless PV inverter connected to the grid, *Proceedings of IEEE APEC*, pp. 907-912, 2007. DOI: 10.1109/APEX.2007.357608.

[22] Bradaschia, F., Cavalcanti, M. C., Ferraz, P. E., Neves, F. A., dos Santos, E. C., and da Silva, J. H., Modulation for three-phase transformerless Z-source inverter to reduce leakage currents in photovoltaic systems, *IEEE Transactions on Industrial Electronics*, vol. 58, no. 12, pp. 5385-5395, 2011. DOI: 10.1109/TIE.2011.2116757.

[23] Xiao, H. and Xie, S., Leakage current analytical model and application in single-phase transformerless photovoltaic grid-connected inverter, *IEEE Transactions on Electromagnetic Compatibility*, vol. 52, no. 4, pp. 902-913, 2010. DOI: 10.1109/TEMC.2010.2064169.

[24] Bhukya, L., Kedika, N. R., and Panda, K. P., A comprehensive review of reduced common-mode voltage modulation techniques for neutral-point-clamped inverters, *IEEE Transactions on Power Electronics*, vol. 38, no. 5, pp. 5769-5790, 2023. DOI: 10.1109/TPEL.2023.3234635.

[25] Orfanoudakis, G. I., Yuratich, M. A., and Sharkh, S. M., Analysis of DC-link capacitor current in three-level neutralpoint-clamped and cascaded H-bridge inverters, *IET Power Electronics*, vol. 6, no. 7, pp. 1376-1389, 2013. DOI: 10.1049/ietpel.2012.0466.

[26] Mondal, S. K., Pinto, J. O., and Bose, B. K., A neural-networkbased space-vector PWM controller for a three-level voltagefed inverter induction motor drive, *IEEE Transactions on Industry Applications*, vol. 38, no. 3, pp. 660-669, 2002. DOI: 10.1109/TIA.2002.1003411.

[27] Das, S., Narayanan, G., and Pandey, M., Space-vector-based hybrid pulse width modulation techniques for a three-level inverter, *IEEE Transactions on Power Electronics*, vol. 29, no. 9, pp. 4580-4591, 2014. DOI: 10.1109/TPEL.2013.2287845.

[28] Subramanian, N. and Stonier, A. A., A Comprehensive Review on Selective Harmonic Elimination Techniques and Its Permissible Standards in Electrical Systems, *IEEE Access*, vol. 12, pp. 141966-141998, 2024. DOI: 10.1109/ACCESS.2024.3436079.

[29] Liu, H., Huang, X., Tan, S., Tse, K. K., and Ruan, X., Switching frequency stabilization methods for adaptive zero-voltageswitching multi-resonant converters, *IEEE Transactions on Power Electronics*, vol. 33, no. 3, pp. 2487-2497, 2018. DOI: 10.1109/TPEL.2017.2697002.

[30] Wang, X., Li, Y., Blaabjerg, F., and Loh, P. C., Virtualimpedance-based control for voltage-source and current-source converters, *IEEE Transactions on Power Electronics*, vol. 30, no. 12, pp. 7019-7037, 2015. DOI: 10.1109/TPEL.2014.2382565.

[31] Zhang, D., Wang, F., Burgos, R., and Boroyevich, D., Impact of interleaving on AC passive components of paralleled three-phase voltage-source converters, *IEEE Transactions on Industry Applications*, vol. 46, no. 3, pp. 1042-1054, 2010. DOI: 10.1109/TIA.2010.2045334.

[32] Kumar, N., Saha, T. K., and Dey, J., Sliding-mode control of PWM dual inverter-based grid-connected PV system: Modeling and performance analysis, *IEEE Journal of Emerging and Selected Topics in Power Electronics*, vol. 4, no. 2, pp. 435-444, 2016. DOI: 10.1109/JESTPE.2015.2497900.

[33] Selvajyothi, K. and Janakiraman, P. A., Extraction of harmonics using composite observers, *IEEE Transactions on Power Delivery*, vol. 23, no. 1, pp. 31-40, 2008. DOI: 10.1109/TPWRD.2007.911190.

[34] Suresh, K., Bharatiraja, C., Chellamuthu, C., and Sanjeevikumar, P., Investigation on embedded controller based solar PVbattery storage system operating modes for residential applications, *Electronics*, vol. 6, no. 4, p. 99, 2017. DOI: 10.3390/electronics6040099.

[35] Ahmed, M., Abdelrahem, M., and Kennel, R., Highly efficient and robust grid connected photovoltaic system based model predictive control with Kalman filtering capability, *Sustainability*, vol. 12, no. 11, p. 4542, 2020. DOI: 10.3390/su12114542.

[36] Rodriguez, J., Kazmierkowski, M. P., Espinoza, J. R., Zanchetta, P., Abu-Rub, H., Young, H. A., and Rojas, C. A., State of the art of finite control set model predictive control in power electronics, *IEEE Transactions on Industrial Informatics*, vol. 9, no. 2, pp. 1003-1016, 2013. DOI: 10.1109/TII.2012.2221469.

[37] Vazquez, S., Leon, J. I., Franquelo, L. G., Rodriguez, J., Young, H. A., Marquez, A., and Zanchetta, P., Model predictive control: A review of its applications in power electronics, *IEEE Industrial Electronics Magazine*, vol. 8, no. 1, pp. 16-31, 2014. DOI: 10.1109/MIE.2013.2290138.

[38] Young, H. A., Perez, M. A., Rodriguez, J., and Abu-Rub, H., Assessing finite-control-set model predictive control: A comparison with a linear current controller in two-level voltage source inverters, *IEEE Industrial Electronics Magazine*, vol. 8, no. 1, pp. 44-52, 2014. DOI: 10.1109/MIE.2013.2294870.

[39] Singh, B., Chandra, A., and Al-Haddad, K., *Power Quality: Problems and Mitigation Techniques*, John Wiley & Sons, London, UK, 2015.

[40] Chen, X., Ruan, X., Yang, D., Zhao, W., and Jia, L., Injected grid current quality improvement for a voltagecontrolled grid-connected inverter, *IEEE Transactions on Power Electronics*, vol. 33, no. 2, pp. 1247-1258, 2018. DOI: 10.1109/TPEL.2017.2678525.

[41] Kazmierkowski, M. P. and Malesani, L., Current control techniques for three-phase voltage-source PWM converters: a survey, *IEEE Transactions on Industrial Electronics*, vol. 45, no. 5, pp. 691-703, 1998. DOI: 10.1109/41.720325.

[42] Sangwongwanich, A., Yang, Y., Blaabjerg, F., and Wang, H., Benchmarking of constant power generation strategies for single-phase grid-connected photovoltaic systems, *IEEE Transactions on Industry Applications*, vol. 54, no. 1, pp. 447-457, 2018. DOI: 10.1109/TIA.2017.2753207.